

PHOTOCHEMICAL AND PHOTOCATALYTIC TRANSFORMATION OF SODIUM BENZOATE BY MEANS OF UV LIGHT AND SUPPORTED TIO₂

Jordi Alan Márquez Jiménez

<https://orcid.org/0000-0002-8512-6010>

Aurelio López Malo-Vigil

<https://orcid.org/0000-0002-8018-5767>

Felipe Córdova Lozano

<https://orcid.org/0000-0001-7517-1953>

Deborah Xanat Flores-Cervantes

<https://orcid.org/0000-0002-0417-9808>

All content in this magazine is licensed under a Creative Commons Attribution License. Attribution-Non-Commercial-Non-Derivatives 4.0 International (CC BY-NC-ND 4.0).



Abstract: The increase in human activities generates additional and more frequent problems related to the availability of water for human consumption. Sodium benzoate is a compound mainly used as a preservative in the food industry, but it has found other applications in fields such as anticorrosive and in medicine as off-label therapeutic agent. Studies have shown that anthropogenic releases of sodium benzoate to the environment have adverse effects on different organisms. This paper presents a study of the process of photochemical transformation of sodium benzoate by exposure to UV and photocatalytic transformation using fixed TiO_2 as a catalyst. We used methodologies with FE-SEM, EDS, UV-Vis Spectroscopy, HPLC and mass spectrometry (MS-MS) to characterize the catalyst and the sodium benzoate transformation products. Such methodologies confirm the formation of transformation products, however, there are no identifiable differences between the products generated by the photochemical and photocatalytic processes. The hydroxylation of sodium benzoate is identified as the main transformation product. Finally, a reaction path is proposed for the generation of the main transformation product with two different oxygen sources, water, and molecular oxygen.

Keywords: Sodium benzoate, photochemical transformation, photocatalysis, TiO_2 , FE-SEM, HPLC.

INTRODUCTION

Currently, water contamination is becoming a major, increasing problem due to the rapid growth and diversification of industrial, agricultural, and household activities which have improved standards of living meaningfully, but have had a negative impact on environment and human health. Water stress and health conditions due to poor quality of water tend to have higher incidences on places where industrial activity is intense (European Environment Agency, 2016). This problem is of greater relevance in countries like Mexico, catalogued as a country with low availability of water (Fondo para la Comunicación y la Educación Ambiental, 2019; CONAGUA, 2018).

Anthropogenic releases of sodium benzoate, considering its use pattern, are expected in surface waters, from industrial or municipal wastewater; and given its physical and chemical properties, the sodium benzoate emitted to water bodies is not expected to volatilize to the atmosphere nor to adsorb to sediment or soil particles. A low to moderate bioaccumulation of sodium benzoate is to be expected (World Health Organization, 2000).

Sodium benzoate is a sodium salt of benzoic acid mainly used as a food preservative, given its antimicrobial properties; the inhibitory action is generally believed to be caused by the encounter of the preservative molecule of a higher pH inside the cell, causing the dissociation of the molecule, thus resulting in the release of charged anions and protons that accumulate inside the cell until the inhibition of microbial cell growth is achieved through a variety of key metabolic reactions inhibitions (Chipley, 2005). Other applications of sodium benzoate include corrosion inhibition (Muzathik et al., 2012) and off-label use as a therapeutic agent to treat acute hyperammonemia in patients with urea cycle disorders (Praphanphoj *et al.*, 2000), hepatic

encephalopathy (Misel *et al.*, 2013) and non-ketotic hyperglycinemia (Walther *et al.*, 1994; Van Hove *et al.*, 2005).

In the United States, sodium benzoate is catalogued as a Generally Recognized as Safe (GRAS) substance up to a maximum permitted level of 0.1%, meaning that it is not subject to premarket review and approval by the FDA because it is generally recognized to be safe under the intended conditions of use with the conclusion of the Selected Committee on GRAS substances that "There is no evidence in the available information on sodium benzoate that demonstrates, or suggests reasonable grounds to suspect, a hazard to the public when they are used at levels that are now current or might reasonably be expected in the future" (Code of Federal Regulations, 1977/1988; FDA, 2019).

It has been proven that in combination with ascorbic acid, sodium benzoate can generate detectable amounts of benzene in aqueous solutions (Chipley, 2005). According to Flores-Guzman *et al.* (2018), sodium benzoate is amongst the chemical agents that can be precursors to cancer. Also, it was proposed by Piper (1999) that extensive ingestion of sodium benzoate, benzoic acid and similar preservatives in the human diet might generate oxidative stress within the epithelia of the gastrointestinal tract, it may contribute to higher incidences of Attention Deficit-Hyperactivity Disorder (Beezhold *et al.*, 2012) and childhood hyperactivity. Some other adverse reactions in other organisms caused by the ingestion of sodium benzoate have been reported, including motor impairment and anxiety in rats (Noorafshan *et al.*, 2014) and induced toxicity and teratogenicity during the early embryonic development of zebrafish (Tsay *et al.*, 2007).

One of the alternatives that has gained researchers interest to carry out the degradation of stable, refractory, organic pollutants in

water is heterogeneous photocatalysis, which is one of the advanced oxidation processes and uses a solid catalyst as the semi-conductor that is activated by a mechanism that involves radical reactive species and generates a series of unselective redox reactions that lead to pollutant degradation (Augugliario *et al.*, 2012; Robert, 2007). There are several semi-conductors used as photosensitizers, for instance Al_2O_3 , ZnO and Fe_2O_3 , however the most widely used is TiO_2 due to its high photocatalytic activity, being not toxic, stable in aqueous solutions and, inexpensive (Garcés-Giraldo *et al.*, 2004)

Immobilizing the TiO_2 in an inert substrate present a series of advantages compared to its use in suspension, reduces turbidity and eliminates the need of photocatalyst filtration processes (Peiró *et al.*, 2000). Amongst the methods to support the TiO_2 are sol-gel method (Portela *et al.*, 2007), spray deposition method (Ranga-Rao & Dutta, 2007), chemical vapor deposition method (Yeung & Lam, 1983), sputtering (Asanuma *et al.*, 2004) and metal-organic chemical vapor deposition (Zhang *et al.*, 2006)

MATERIALS AND METHODS

SYNTHESIS OF CATALYST

SUBSTRATES

Borosilicate glass slides (2.5x2.5 cm) were used as substrates and thoroughly washed with soap and water and rinsed with distilled water. Subsequently, they were introduced to an ethanol solution and cleaned for 10 minutes in a Cole-Parmer 8890 ultrasonic cleaner, repeating the process with acetone. Finally, the substrates were introduced to a FE-291AD oven at 120°C and let to dry.

REAGENTS

The chemicals used in this section were reagent grade and were used without further

purification: Titanium (IV) isopropoxide (TTIP, Sigma-Aldrich, Toluca, Mexico), absolute ethanol (EtOH, Merck, Darmstadt, Alemania), polyvinylpyrrolidone (PVP, Golden bell, Jalisco, Mexico), acetic acid (Avantor, Estado de México, Mexico). The water used in all preparations was provided by Ecopura® (Puebla, Mexico).

PREPARATION OF AQUEOUS COLLOIDAL SOLUTION

The synthesis of TiO₂ nanoparticles was carried out *in situ* through a sol-gel process. PVP (0.2 g) was dissolved in absolute EtOH (3 ml), the solution was subjected to ultrasonic bath (15 min) and moderate agitation afterwards until a homogeneous, transparent solution was achieved. A second solution was prepared using absolute EtOH (3 ml), acetic acid (1.5 ml) and TTIP (0.75 ml) and subjected to moderate agitation (30 min). Both solutions were preserved from atmospheric moisture. The latter solution was mixed with the former through a drop-wise addition under moderate agitation. The resulting solution was subjected to moderate agitation while preserved from ambient moisture.

DEPOSITION METHOD

For film preparation, a standard static dispense spin coating technique was used, injecting 75 ml to the surface of the substrate, assuring an even application across the surface, a spin speed of 4000 rpm was applied and a duration of 30 seconds to guarantee that the solvent evaporated completely using a CHEMAT TECHNOLOGY KW-4A Spin Coater 110V. Subsequently, the substrates were introduced to a muffle furnace model Thermo Scientific Thermolyne 5.8L D1 Benchtop at 100°C for a period of 15 minutes. This process was repeated for a total of four depositions. After the final deposition, the temperature inside the muffle furnace was

gradually incremented to 400°C; temperature at which the substrates remained for a period of 4 hours.

CHARACTERIZATION TECHNIQUE

Characterization of the surface morphology of the nanoparticles deposited on the borosilicate glass substrates by Field Emission Scanning Electron Microscopy (FE-SEM) was carried out with a ultra-high resolution FE-SEM, TESCAN model MAIA 3 2017 operated at 10 kV acceleration voltage and with in-beam Secondary Electron (SE) detection. To confirm the presence of the catalyst across the substrate, an additional Energy Dispersive X-Ray Spectroscopy (EDS) microanalysis was performed using the equipment aforementioned, operated at 15 kV acceleration voltage. All samples were coated with an ultra-thin layer of gold through a sputtering deposition method prior to their analysis to create a conductive layer, improving the imaging of the samples by the inhibition of charges, reduction of thermal damage and improving the secondary electron signal. The equipment used was a SEC MCM-100: Ion Sputter Coater for Non-Conductive Samples.

To test the wear resistance of the catalyst, the substrates were introduced to beakers containing 5 ml of distilled water and submitted to ultrasonication for 1 and 2 min. The liquid samples were then filtered through a 0.2 mm nylon filters and a vacuum filtration system. Finally, the filters, previously sputter-coated with gold, were analyzed by means of a FE-SEM.

TRANSFORMATION OF SODIUM BENZOATE

SAMPLE PREPARATION

Solutions of 20 ml of Sodium benzoate (Meyer®, Ciudad de México, Mexico) were prepared dissolving sodium benzoate powder

with deionized water provided by Ecopura® at room temperature and introduced in 50 ml borosilicate glass beakers.

PHOTOLYSIS AND PHOTOCATALYSIS

Sodium benzoate solutions at different concentrations were irradiated with UV through a TIMCO Est professional sterilizer (46X21X20 cm) consisting on a 28W medium-pressure mercury vapor lamp. An UVP Model UVX Digital Radiometer was used to determine the ultraviolet intensity from the lamps used, taking repeated measures over a period of 3 hours to ensure stable intensity, which was defined to be 16,500 and 18,000 mW/cm², respectively, for the two lamps used. The photoactivity of TiO₂ films on glass slides was evaluated by the degradation of 10 ppm methylene blue (Sigma Aldrich, Toluca, Mexico) solutions under UV illumination.

CHARACTERIZATION OF TRANSFORMATION PRODUCTS

UV-VIS SPECTROPHOTOMETRY

The proposed method was developed using monochromator-based optical system Thermoscientific UV-Vis spectrophotometer model Multiskan Sky with touchscreen and cuvette, using 10 mm path length quartz cuvettes. All determinations were made through a scan ranging between 200 nm to 300 nm wavelength. All weighings were done on an Ohaus® analytical balance model Pioneer Plus Analytical PA224C with a readability of 0.1 mg. Glassware used in each procedure were washed with detergent and rinsed thoroughly with distilled water and dried in a hot air oven.

To determine the correlation or lack thereof between the UV light exposition time and the absorbance of the samples, sodium benzoate solutions at different concentrations (20, 200, 500, 800 and 1000 ppm) were submitted

to UV irradiation, whose exposure time was set at 23 h, taking spectrophotometric determinations of the samples every hour at 271 nm wavelength. Additionally, a spectrophotometric scan ranging from 200 nm to 300 nm wavelength was carried out for sodium benzoate solutions in concentrations of 1000 ppm in the presence and absence of the TiO₂ catalyst and for an exposition time of 24 hours.

HIGH-PERFORMANCE LIQUID CHROMATOGRAPHY (HPLC)

For the analysis of the transformation of sodium benzoate, the proposed method, adapted from Khade and Mirgane (2014), was conducted using the reversed phase technique using an Agilent Technologies 1260 Infinity HPLC system, consisting on a degasser, a G1311B 1260 quaternary pump, a G1329B 1260 ALS standard auto-sampler with thermostat, a G1362A 1260 RID refraction index detector monitoring at 254 nm, a G4212B 1260 DAD diode array detector, and a G1316A 1260 TCC thermostatted column compartment. The analyte peaks were resolved at the ambient temperature on a ZORBAX Eclipse XDB-C18 (4.6 x 100 mm, particle size 3.5 µm) column. The volume of the injection loop was 20 µl.

The data were collected and analyzed with a ChemStation software. Chromatographic conditions were as follows:

- Volumetric flow: 1 ml/min
- Detection: 254 nm
- Injection volume: 20 µl
- Testing time: 10 min

The preparation of the buffer consisted on the dissolution of 6.8 g of potassium dihydrogen ortho phosphate (J.T Baker, Estado de México, Mexico) in 1000 ml distilled water. The dissolution was filtered through 0.45-micron Nylon membrane filter paper and degassed with ultrasonic bath for

5 minutes. The mobile phase was prepared by mixing the buffer solution with HPLC-grade methanol (Avantor, Estado de México, Mexico) in a 60:40 v/v ratio and degassing it with an ultrasonic bath for 5 to 10 minutes using a Branson 2800 ultrasonic bath equipment. Samples diluted on a ratio 1:100 from the previous section were subjected to this analysis.

MASS SPECTROMETRY (MS-MS)

The analytical method was adapted from one previously reported by Ling *et al.* (2017). Samples were injected at 5 mL volumes and were loaded onto an XBridge (Waters) C-18 Intelligent Speed (2.1 mm × 20 mm, particle size 5 μm) trap column. Elution from the trap column and onto an XBridge (Waters) C-18 analytical column (2.1 mm × 50 mm, particle size 3.5 μm) was performed using a gradient pump delivering 200 μL min⁻¹ of a water and MeOH mobile phase, each containing 0.1 vol % formic acid. The HPLC-MS was operated with electrospray ionization in positive and negative polarity modes. The MS acquired full-scan MS data within a mass-to-charge range of 100–1000 for each sample followed by a data-dependent acquisition of product ion spectra (MS/MS).

RESULTS AND DISCUSSION

TiO₂ THIN-FILM CHARACTERIZATION

Preliminary work has shown that PVP can be used as an agglomeration controller agent and also as particle size regulator; in this work PVP K-30 was used. Other uses of PVP in TiO₂ deposition methods are reported in the literature (Laamari *et al.*, 2016). The attainment of initial good adherence of the TiO₂ film to the substrate suggests that strong joining forces action are present between the substrate and the deposited crystallites. The existence of strong covalent oxo bridges

((>X-O-Ti<;X) Si, Sn) could account for the adherence presented.

Morphology and size of colloidal nanoparticles were examined by FE-SEM. Figure 1 shows the quasi-spherical structure of the TiO₂ particles in the thin film with a particle diameter ranging between 60 nm and 114 nm.

The amount of TiO₂ deposited in each process is small, as estimated by gravimetry: a 4-fold spin-coated glass substrate contains approximately 22.4×10^{-2} mg of TiO₂ cm⁻², i.e., a layer thickness of 4.06 nm, considering the whole layer as being compact as observed in Figure 2.

XDS microanalysis performed in several points across the substrate revealed the presence of TiO₂ in the surface of the glass. The TiO₂ was homogeneously distributed except from some isolated areas that presented layer cracking. Figure 3 a) shows the analysis of a crack in the substrate, whilst 3 b) shows the result of the XDS analysis of a section of the substrate with deposit. Confirming the absence of TiO₂ in the layer cracks. It is possible to suspect that the fissures are caused by the elevated annealing temperatures. However, when subjected to ultrasonication, the filters from the water in contact with the substrates contained very little material, indicating good stability.

CHARACTERIZATION OF DEGRADATION OF SODIUM BENZOATE

UV-VIS SPECTROPHOTOMETRY

Figure 4 shows the plots obtained from the absorbance measurement at a wavelength of 271 nm carried out to sodium benzoate solutions at different concentrations, where blue dots represent the absorbance of the samples exposed to UV light and the orange dots represent the values obtained for the blank solutions. It is

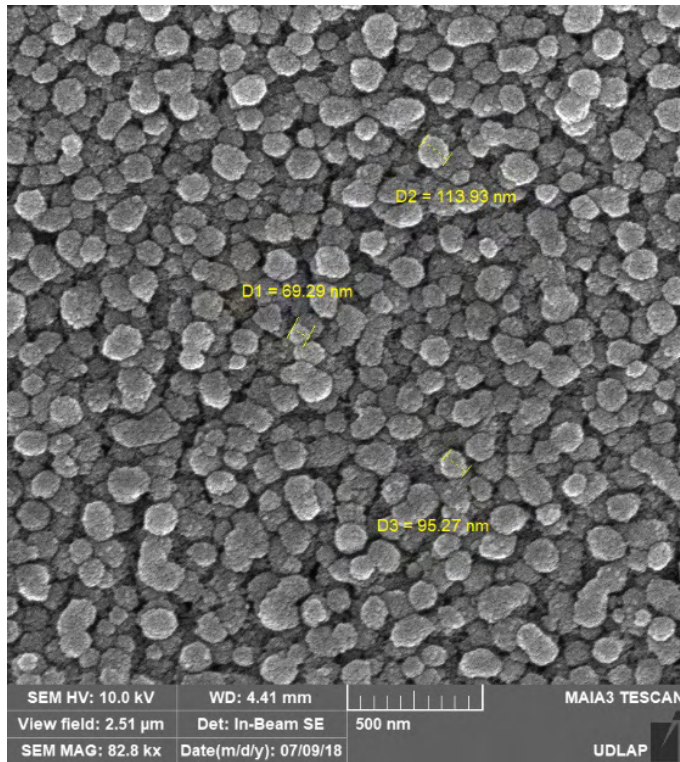


Figure 1. FE-SEM plain-view image of a borosilicate glass substrate spin-coated with 4 layers of TiO_2 @4000 rpm

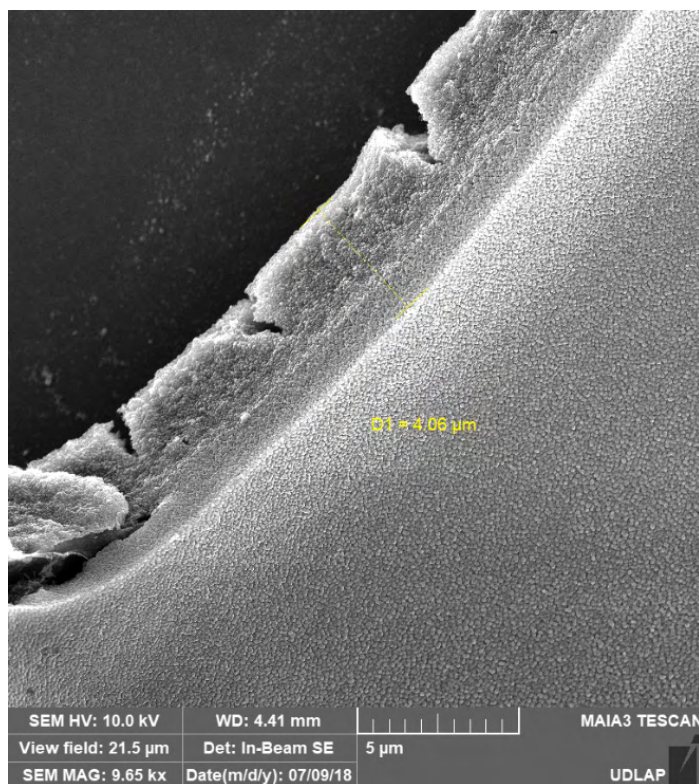


Figure 2. FE-SEM cross sectional view image of a borosilicate glass substrate spin-coated with 4 layers of TiO_2 @4000 rpm

possible to observe an acceptable correlation between the factors plotted (exposition time to UV light, in hours and absorbance) having a maximum R^2 value of 0.97.

HIGH-PERFORMANCE LIQUID CHROMATOGRAPHY (HPLC)

Two different treatment procedures were evaluated, photochemical transformation through the exposure to UV light and photocatalytic transformation of the sodium benzoate using fixed TiO_2 as catalyst. Figure 5 displays the resulting spectrophotometric scan besides the blank (initial) solution after 24 hours of treatment carried out as mentioned in the materials and methods section.

All three scans show two common absorption peaks highlighted in the plots with a red circle, corresponding to wavelengths of 300 nm and 250 nm; there is also an absorption peak common in the treated samples but not present in the initial, untreated sodium benzoate at a wavelength of 271 nm, which may correspond to the absorbance of the transformation products. These absorbance peaks are highlighted in the plots with a green circle. The total of absorption peaks reported correspond to the UVC range of the ultraviolet electromagnetic spectrum.

HIGH-PERFORMANCE LIQUID CHROMATOGRAPHY (HPLC)

A run in the HPLC system was carried out to track the formation of the suspected transformation products. The determination of a pure, untreated sample of sodium benzoate was analyzed to obtain the baseline chromatogram. Following, samples after different UV light exposure times were analyzed. A total analysis of sodium benzoate was completed in less than 10 minutes. In the base line chromatogram it is possible to observe a peak at a retention time of 1.258 minutes, which corresponds to sodium benzoate. This peak presents an approximately

Gaussian form, and does not present tailing nor fronting profiles.

Figure 6 shows a representation of the chromatograms obtained for the sodium benzoate samples after different UV exposition times alongside the baseline chromatogram for the untreated sample. The formation and evolution of two additional peaks at retention times of around 0.903 min and 1.03 min, respectively, not corresponding to the baseline peak attributed to the sodium benzoate can be observed. Additionally, Table 1 displays the area and retention time for the three peaks observed in the chromatogram, showing that the two peaks not ascribable to the sodium benzoate present an increasing area dependent on UV exposure time; it can also be seen that the retention time for such peaks remains constant.

As observed in Figure 7, there is no perceivable difference in the profile nor the retention times of the different peaks of the chromatograms generated from samples undergoing photochemical and photocatalytic treatment processes, indicating that no different compounds are generated in each treatment.

MASS SPECTROMETRY (MS-MS)

Figure 8 depicts a mass chromatogram and a mass spectrum for a sodium benzoate untreated sample, and it can be observed that the peak corresponding to sodium benzoate has a retention time of 12.4 minutes. The mass spectra was captured within the obtained peak and shows the characteristic mass of the deprotonated form of benzoic acid. There is also evidence of the ^{13}C monoisotopic peak at $m/z = 122.0313$.

Figure 9 represents the corresponding chromatogram and mass spectra for a treated sample. Here it can be seen the same peak at the same retention time of 12.4 minutes corresponding to the sodium benzoate, but a new, secondary peak seems to be emerging

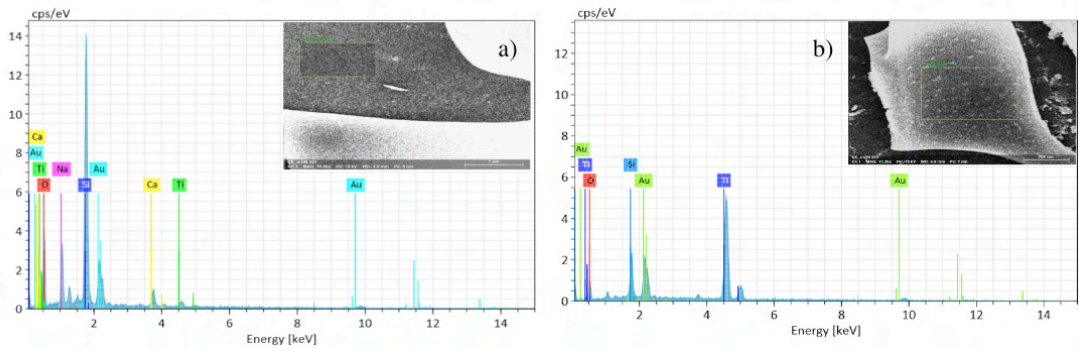


Figure 3. XDS microanalysis of a substrate of a deposit crack (left) and the thin film (right)

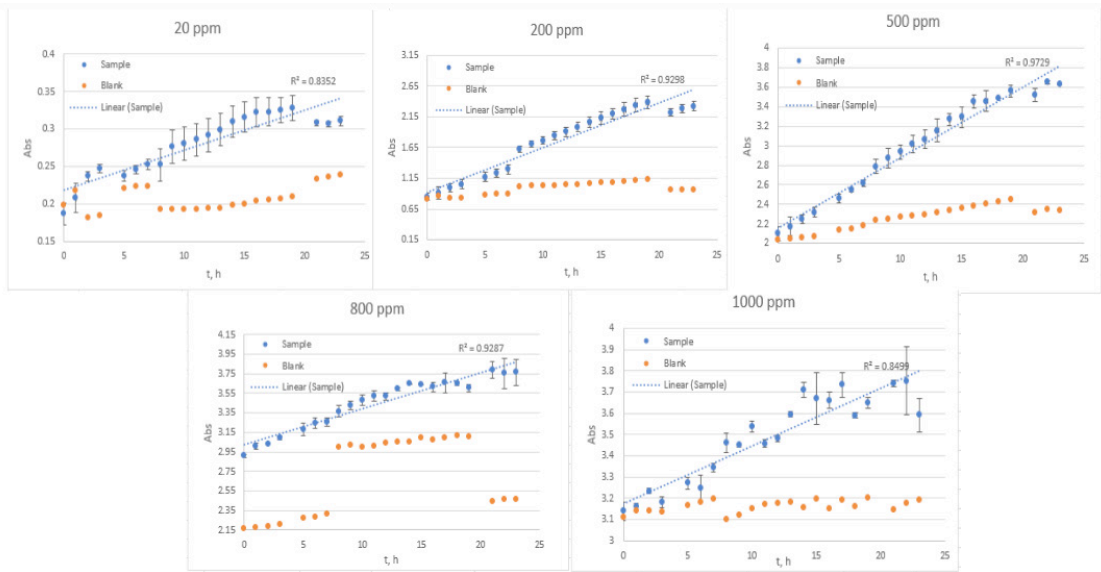


Figure 4. UV-Vis absorbance measurements at different NaB concentrations (top, from left to right 20, 200 and 500 ppm); (bottom, from left to right, 800 and 1000 ppm) @271 nm wavelength

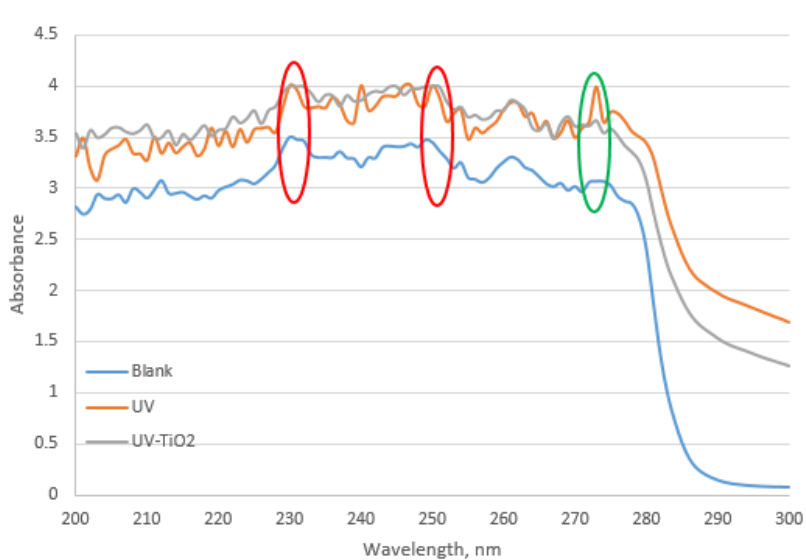


Figure 5. UV-vis absorption spectra of absorbance versus wavelength (200-300 nm) for NaB samples after 24 h treatments

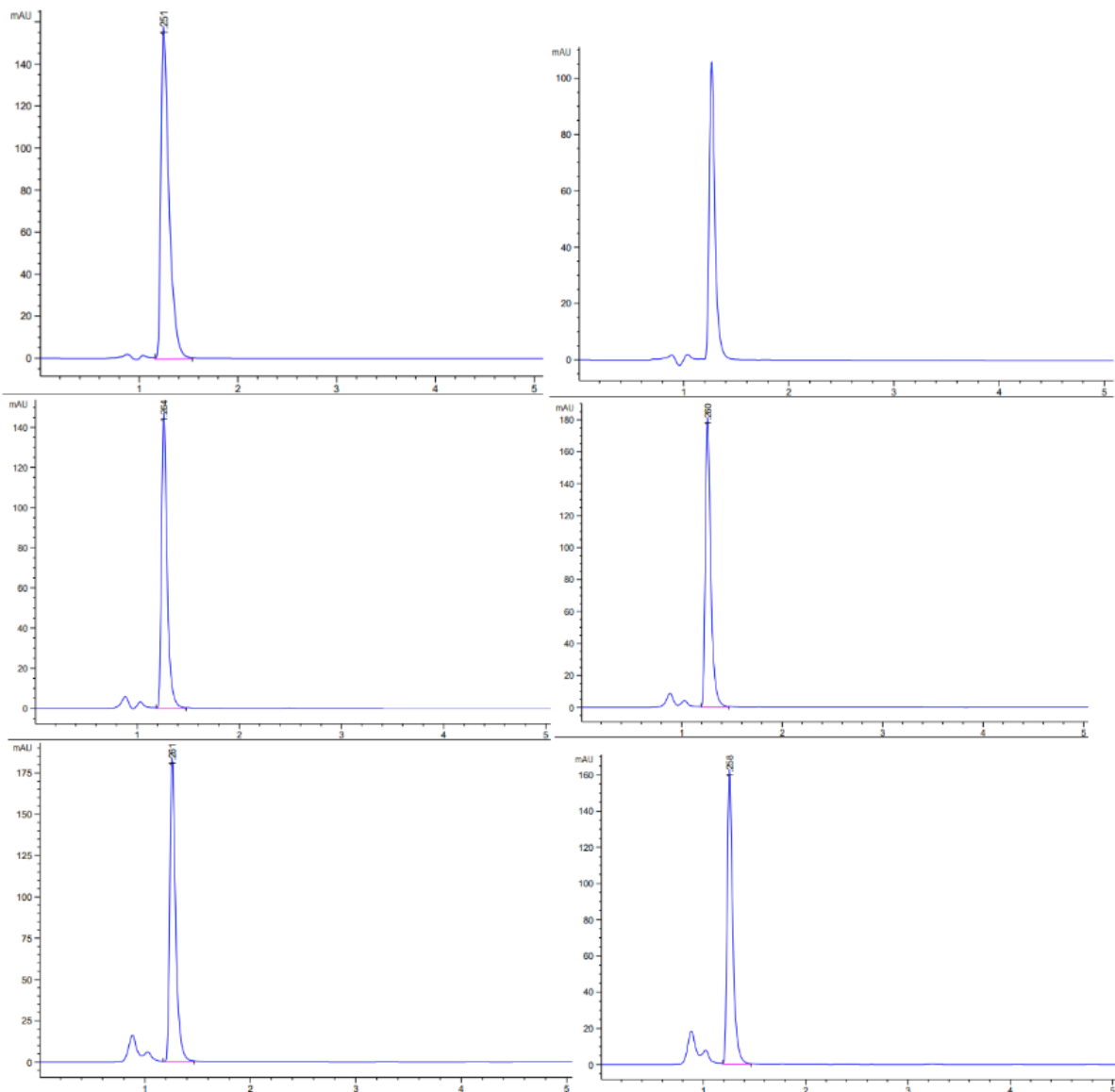


Figure 6. HPLC chromatograms for sodium benzoate samples at different UV exposition times (from left to right and top to bottom, 0 h, 4h, 8 h, 12 h, 16 h and 24 h)

		Area, mAU*s			Retention t, min		
Sample	t _{exposition} , h	Peak 1	Peak 2	Peak 3	Peak 1	Peak 2	Peak 3
1	0	9.26388	3.6105	374.00806	0.964	1.025	1.161
2	0	10.82855	3.45343	573.80115	0.962	1.037	1.260
Average		10.046215	3.531965	473.904605	0.963	1.031	1.2105
Stdev		1.10638877	0.11106526	141.275049	0.00141421	0.00848528	0.07000357
3	4	10.11981	3.38148	395.15976	0.958	1.040	1.266
4	4	14.48536	5.65	568.45782	0.887	1.036	1.264
Average		12.302585	4.51574	481.80879	0.9225	1.038	1.265
Stdev		3.08691001	1.60408588	122.540233	0.05020458	0.00282843	0.00141421
5	8	26.11768	14.38971	552.15582	0.885	1.032	1.263
6	8	38.14803	14.86545	740.70056	0.886	1.032	1.262
Average		32.132855	14.62758	646.42819	0.8855	1.032	1.2625
Stdev		8.50674207	0.33639898	133.321264	0.00070711	0	0.00070711
7	12	33.53674	12.48496	688.21997	0.886	1.028	1.260
8	12	35.51665	12.55604	782.48303	0.885	1.030	1.259
Average		34.526695	12.5205	735.3515	0.8855	1.029	1.2595
Stdev		1.40000779	0.05026115	66.6540489	0.00070711	0.00141421	0.00070711
9	16	86.76578	32.56644	701.60547	0.883	1.027	1.260
10	16	66.61835	26.18209	640.50116	0.883	1.028	1.260
Average		76.692065	29.374265	671.053315	0.883	1.0275	1.26
Stdev		14.2463844	4.51441718	43.207272	0	0.00070711	0
11	24	93.42172	29.41121	610.46692	0.884	1.024	1.257
12	24	133.60381	48.60559	602.15002	0.88	1.023	1.255
Average		113.512765	39.0084	606.30847	0.882	1.0235	1.256
Stdev		28.4130283	13.5724763	5.88093639	0.00282843	0.00070711	0.00141421

Table 1. Peak area and retention time for sodium benzoate samples at different UV exposition times.

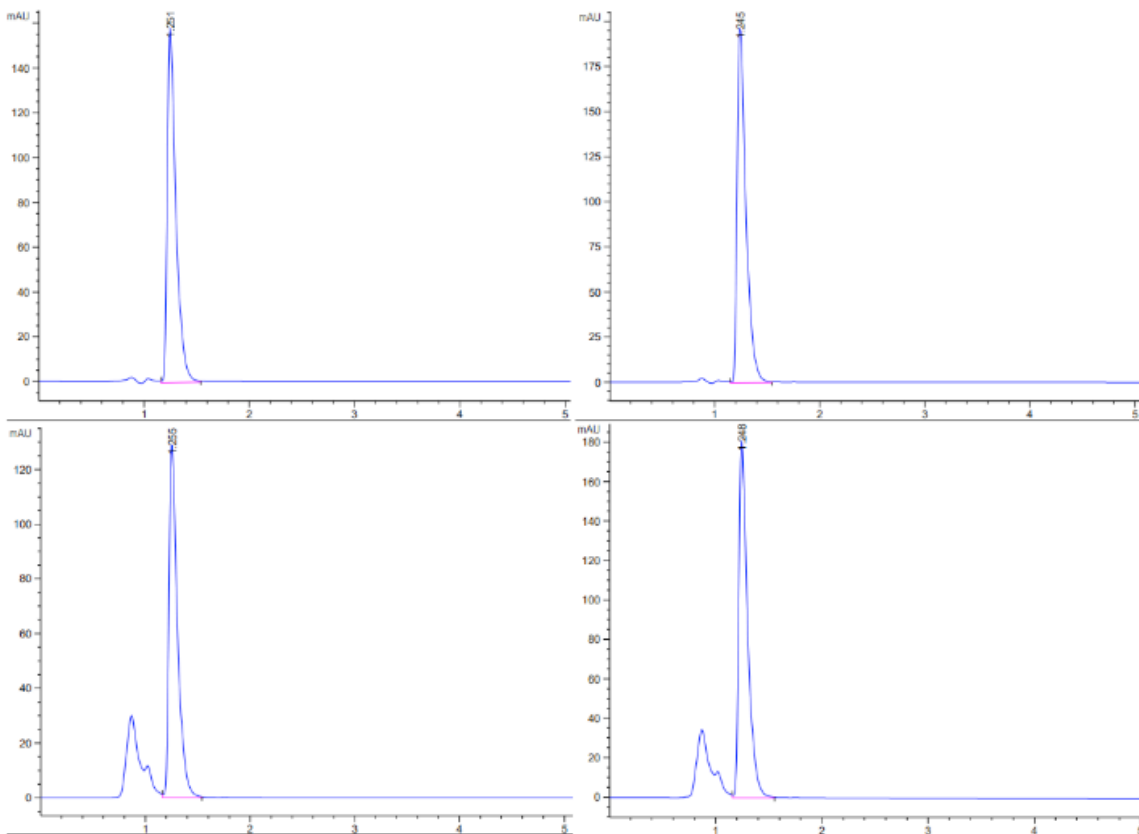


Figure 7. Chromatograms after 24 h of treatment (from left to right and top to bottom, blank sample without catalyst, blank sample with catalyst, photochemical treatment and photocatalytic treatment)

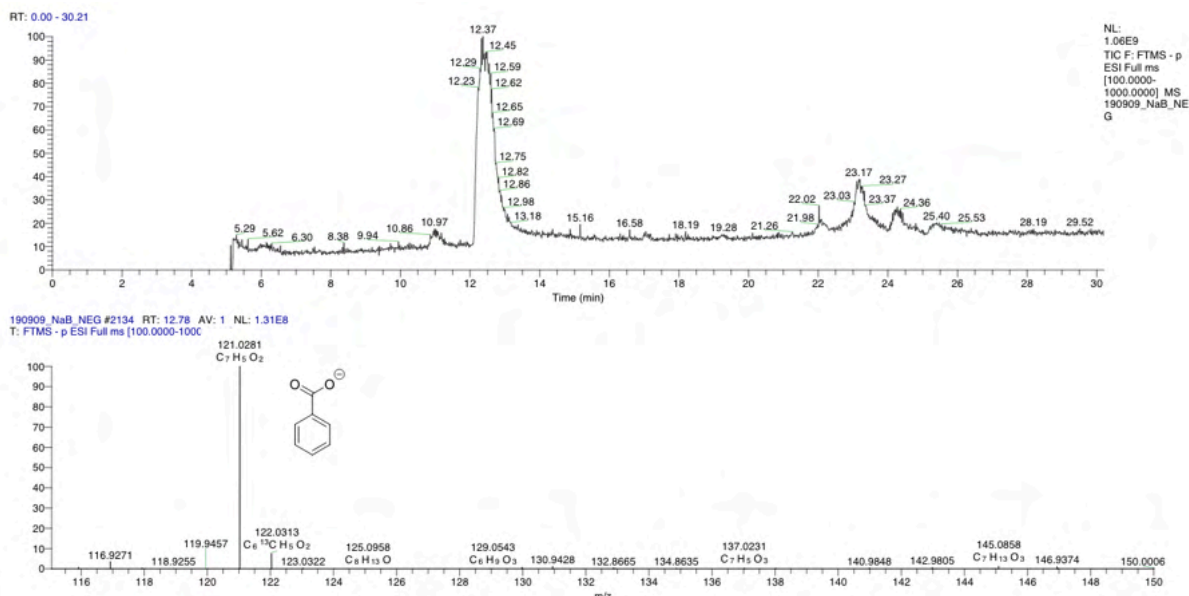


Figure 8. Mass chromatogram (top) and mass spectra (below) of untreated sodium benzoate sample.

from the original peak at a retention time of 12.8 minutes, highlighted in the figure with a red circle; also, minor peaks appear at retention times of 14.2 and 14.8 minutes. From the mass spectra, captured at the peak with a retention time of 12.8 minutes, it can be seen the characteristic mass of the deprotonated form of benzoic acid, along with a mass previously not present of 137.0233 that may correspond to a monohydroxylated benzoic acid. There is also evidence of the ^{13}C monoisotopic peaks at $m/z = 122.0313$ and $m/z = 138.0266$, respectively.

Considering that the peak corresponding to the 137.0233 mass is not present when a mass spectrum is obtained at retention times under 12.4, it is possible to confirm the presence of a new chemical present in the treated sample. The Normalization Level (NL) of $3.09\text{E}8$ of such peak relative to the intensity of the peak for the sodium benzoate in the untreated sample ($1.31\text{E}8$) suggest that the monohydroxylated benzoic acid is the major transformation product.

Figure 10 represent the reaction pathway proposed for the transformation of sodium benzoate, suggesting that the transformation product is produced as a result of reaction between the sodium benzoate or benzoic acid and an OH^* radical, which is produced by the oxidation of a $-\text{OH}$ group on the catalyst surface or the solution by a photogenerated hole. Similar to that reported by Bui *et al.* (2010) for the oxidation of benzene, two different oxygen sources can be proposed: water and molecular oxygen. The pathway using water as the oxygen source is ascribed to oxygen transfer in the initial oxidation of the sodium benzoate oxidation, whilst the process involving molecular oxygen as the oxygen source can be attributed to the hole transfer process in the initial oxidation of the molecule. As stated by Auguglaro *et al.* (2012) cation radicals, which are formed by the hole transfer mechanism, are the species that react with

oxygen. The peroxide radical formed because of the reaction between the benzene cation radical and an O_2 molecule can be converted to phenol through reductive processes.

Figure 11 shows a mass spectra obtained at a retention time of 14.2 minutes for both the untreated and the treated samples, where it is possible to note that the spectrum at 241.0505 is clearly present only in the treated sample, suggesting a minor transformation product, a structure for such product is also proposed based on the mass obtained.

CONCLUSIONS

Given the observed correlation between UV exposure and absorbance, we conclude that, contrary to what is reported in the literature (World Health Organization, 2000), sodium benzoate is photosensitive and thus, can undergo chemical reactions in the presence of a photo induced excitation of the molecule.

No significant difference was observed with the two treatment procedures followed, indicating that sodium benzoate may be reacting with free radicals, mainly hydroxyl radicals generated by the absorption of photons. The data obtained through the MS-MS analysis of the transformation product, specifically regarding the one identified as the main transformation product cannot resolve whether the $-\text{OH}$ group is added in the ortho-, metha- or para- position, nonetheless, based on the oxidation mechanism reported for similar compounds such as dichlorobenzene, it can be proposed that the primary attack of hydroxyl radical generates its regioselective insertion in the meta position.

Further studies on the characterization and properties determination such as toxicity and color of the sodium transformation products are required to determine the viability of the processes used in this paper as a treatment alternative for sodium benzoate aqueous releases.

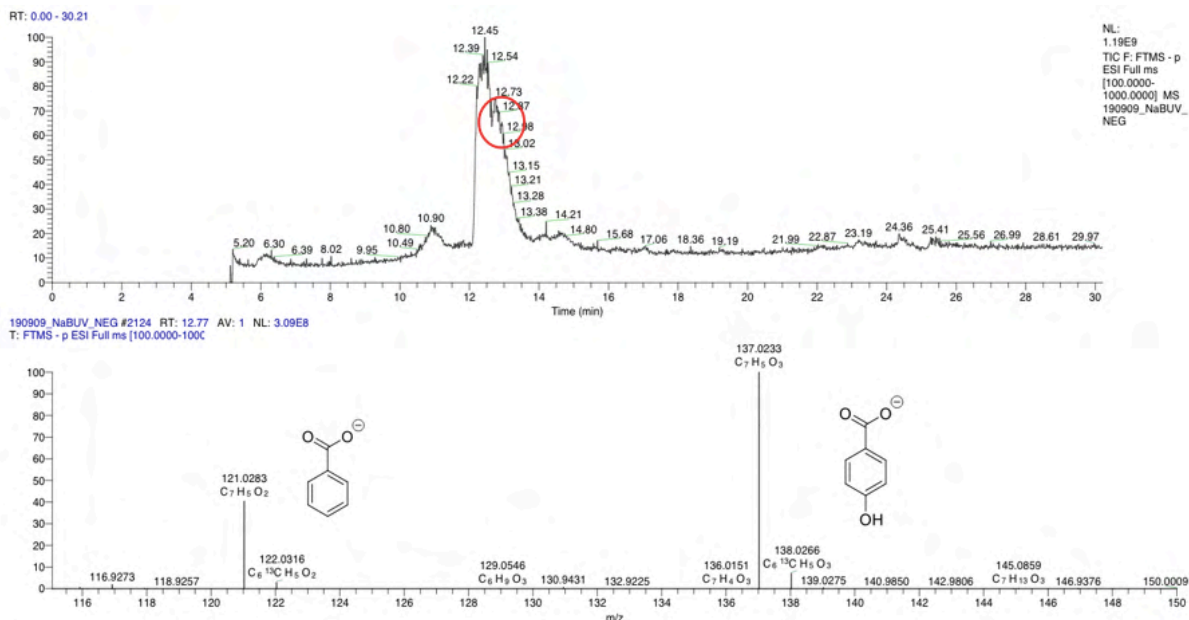


Figure 9. Mass chromatogram (top) and mass spectra (below) of a treated sodium benzoate sample.

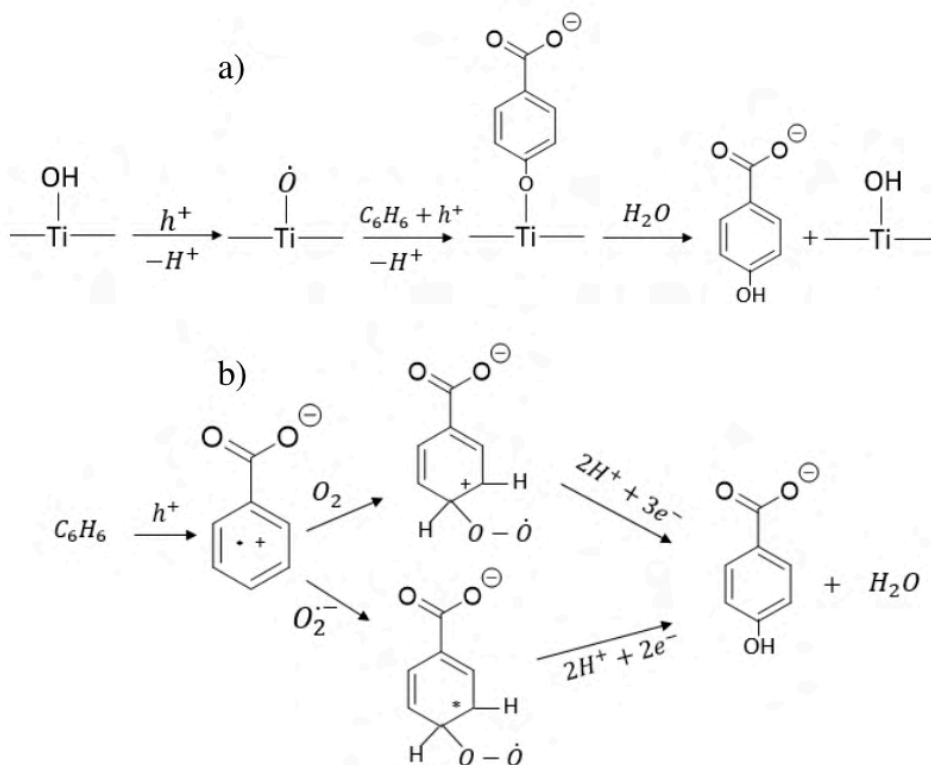


Figure 10. Mechanism for production of main transformation product from sodium benzoate/benzoic acid through an oxygen transfer process using: (a) water (b) O₂ as oxygen source.

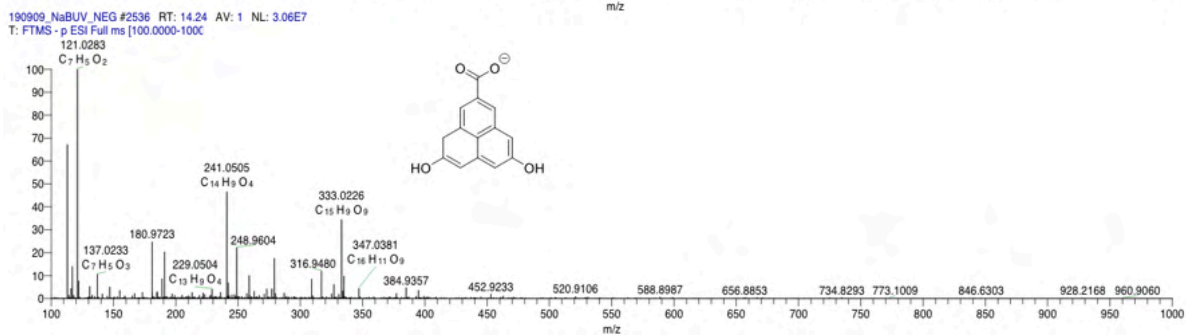
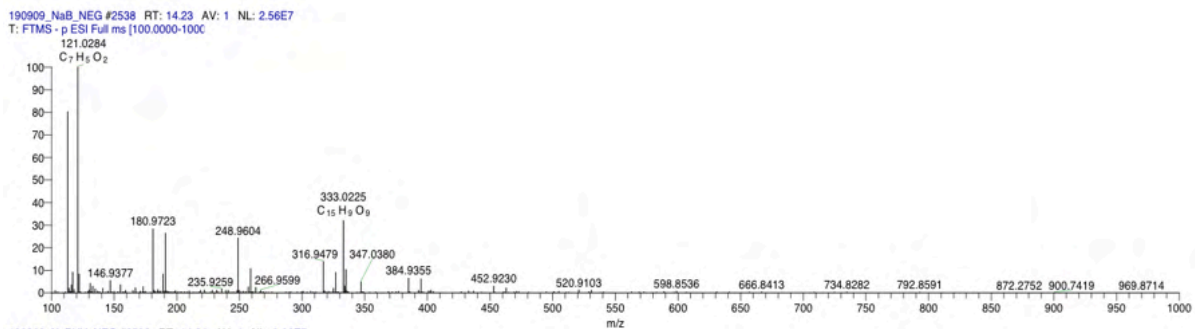


Figure 11 Mass spectra at retention time of 14.2 minutes for untreated sample (top) and treated sample (bottom).

REFERENCES

- Asanuma, T., Matsutani, T., Liu, C., Mihara, T., & Kiuchi, M. (2004). **Structural and optical properties of titanium dioxide films deposited by reactive magnetron sputtering in pure oxygen plasma.** *Journal of Applied Physics*, 95(11), 6011–6016. doi:10.1063/1.1728313
- Augugliaro, V., Bellardita, M., Loddo, V., Palmisano, G., Palmisano, L., & Yurdakal, S. (2012). **Overview on oxidation mechanisms of organic compounds by TiO₂ in heterogeneous photocatalysis.** *Journal of Photochemistry and Photobiology C: Photochemistry Reviews*, 13(3), 224–245. doi:10.1016/j.jphotochemrev.2012.04.00
- Beezhold BL, Johnston CS, Nochta KA. **Sodium Benzoate Rich Beverage Consumption is Associated With Increased Reporting of ADHD Symptoms in College Students: A Pilot Investigation.** *J Atten Disord* 2012; 25.
- Bui, T.D., Kimura, A., Ikeda, S. and Matsumura, M. (2010). **Determination of Oxygen Sources for Oxidation of Benzene on TiO₂ Photocatalysts in Aqueous Solutions Containing Molecular Oxygen.** *J. Am. Chem. Soc.* 2010, 132, 24, 8453-8458
- Code of Federal Regulations. (1977/1988). **Title 21.** Parts 100-199, Food and Drugs, U.S. Government Printing Office, Washington, D.C.
- CONAGUA. (2018). **Atlas del agua en México 2018.** Sistema Nacional de Información del Agua.
- Chipley, J. (2005). **Chapter 2: Sodium Benzoate and Benzoic acid.** In P. Michael-Davidson, J. Sofos & A. Branen (Eds.). *Antimicrobials in food (3rd ed.)*. (pp. 11-48). Boca Raton , FL: Taylor and Francis Group
- European Environment Agency. (2016). **Environmental signals 2000-** Environmental Assessment Report No. 6.
- FDA. (2019). **Selected Committee on GRAS Substances.** [database].
- Fondo para la Comunicación y la Educación Ambiental. (2019). **Visión general del agua en México.**
- Flores-Guzmán, F., Hernández-Vázquez, J. & Carrasco-Ramírez, E. (2018). **La contaminación ambiental como factor inductor de diabetes y cáncer.** In V. Avila-Akerberg, I. Vizcarra-Bordi & T. González-Martínez (Eds.). *Sustentabilidad ambiental. Una visión interdisciplinaria de los DAAD-Alumni en México.* (pp. 51-66). México
- Garcés Giraldo, L., & Mejía Franco, E., & Santamaría Arango, J. (2004). **La fotocatalisis como alternativa para el tratamiento de aguas residuales.** *Revista Lasallista de Investigación*, 1 (1), 83-92
- Khade, V. y Mirgane , S. (2014). **High-performance liquid chromatography method for the analysis of sodium benzoate.** *International Journal of Scientific & Engineering Research*, Volume 5, Issue 10, October-2014 ISSN 2229-5518.
- Laamari, M., Ben-Youssef, A. & Bousselmi, L. (2016). **Electrophoretic deposition of titanium dioxide films on copper in aqueous media.** *Water Sci Technol.* 2016;74(2):424-30. doi: 10.2166/wst.2016.197.
- Misel, M. L., Gish, R. G., Patton, H., & Mendler, M. (2013). **Sodium benzoate for treatment of hepatic encephalopathy.** *Gastroenterology & hepatology*, 9(4), 219–227.
- Muzathik, A.M, Ahmad, M.F, Kamales, B. & Wan Nik, W.B. (2012). **Sodium benzoate as corrosion inhibitor for aluminum alloy AA 7618 in tropical seawater.** MARTEC 2012 International Conference, Malaysia.
- Noorafshan, A., Erfanzadeh, M. & Karbalay-Doust, S. (2014). **Sodium benzoate, a food preservative, induces anxiety and motor impairment in rats.** *Neuroscience Journal*, 19(1), 24-28.
- Peiró, A.M., Peral, J., Domingo, C., Domènech, X., & Ayllón, J.A. (2001). **Low-Temperature Deposition of TiO₂ Thin Films with Photocatalytic Activity from Colloidal Anatase Aqueous Solutions.** *Chem. Mater.* 13, 2567-2573
- Piper, P. W. (1999). **Yeast superoxide dismutase mutants reveal a pro-oxidant action of weak organic acid food preservatives.** *Free Radic. Biol. Medic.* 27:1219
- Portela, R., Sánchez, B., Coronado, J.M., Candal, R., & Suárez, S. (2007). **Selection of TiO₂-support: UV- transparent alternatives and long-term use limitations for H₂S removal.** *Catalysis Today.* 129, 223-230

- Praphanphojj, V., Boyadjiev, S.A, Waber, L.J, Brusilow, S.W & Geragthy, M.T. (2000). **Three cases of intravenous sodium benzoate and sodium phenylacetate toxicity occurring in the treatment of acute hyperammonaemia.** *J. Inherit. Metab. Dis.* 23. 129-136
- Ranga-Rao, A. & Dutta, V. (2007). **Low-temperature synthesis of TiO₂ nanoparticles and preparation of TiO₂ thin films by spray deposition.** *Solar Energy Materials & Solar Cells.* 91, 1075-1080
- Robert, D. (2007). **Photosensitization of TiO₂ by MxOy and MxSy nanoparticles for heterogeneous photocatalysis applications.** *Catalysis Today*, 122(1-2), 20–26. doi:10.1016/j.cattod.2007.01.060
- Tsay, H.-J., Wang, Y.-H., Chen, W.-L., Huang, M.-Y., & Chen, Y.-H. (2007). **Treatment with sodium benzoate leads to malformation of zebrafish larvae.** *Neurotoxicology and Teratology*, 29(5), 562–569. doi:10.1016/j.ntt.2007.05.001
- Van Hove, J.L., Vande Kerckhove, K., Hennermann, J.B., Mahieu, V., Declercq, P., Mertens, S., De Becker, M., Kishnani, P.S. & Jaeken, J. (2005). **Benzoate treatment and the glycine index in nonketonic hyperglycinaemia.** *J. Inherit. Metab. Dis.* 28(5):651-63.
- Walther, F., Radke, M., Kruger, G., Hobusch, D., Uhlemann, M., Tittelbach-Helmrnich, W. & Stolpe, H.J. (1994). **Response to sodium benzoate treatment in non-ketonic hyperglycinaemia.** *Acta. Paediatr. Jpn.* 36:75-79.
- World Health Organization. (2000). **Concise International Chemical Assessment Document 26, Benzoic acid and Sodium benzoate**, Geneva
- Yeung, K.S. & Lam, Y. W. (1983). **A simple chemical vapour deposition method for depositing thin TiO₂ films.** *Thin Solid Films.* 109, 169-178
- Zhang, X., Zhou, M., & Lei, L. (2006). **Co-deposition of photocatalytic Fe doped TiO₂ coatings by MOCVD.** *Catalysis Communications*, 7(7), 427–431. doi:10.1016/j.catcom.2005.12.023